Liquid metal as a broadband saturable absorber for passively *Q*-switched lasers

Tianqi Zhang (张天琦)[1,2], Mudong Wang (王木东)[1,2], Yang Xue (薛 杨)[1,2], Jinlong Xu (徐金龙)[3,*], Zhenda Xie (谢臻达)[3,], and Shining Zhu (祝世宁)[2]**

[1]*National Laboratory of Solid State Microstructures, Nanjing University, Nanjing 210093, China*
[2]*School of Physics, Nanjing University, Nanjing 210093, China*
[3]*School of Electronic Science and Engineering, Nanjing University, Nanjing 210093, China*
**Corresponding author: longno.2@163.com; **corresponding author: xiezhenda@nju.edu.cn*
Received June 15, 2020; accepted July 23, 2020; posted online September 17, 2020

We demonstrated the efficient plasmon-induced nonlinear absorption of liquid metal GaInSn nanospheres prepared by a facile liquid-phase method. With GaInSn as saturable absorbers, a passively *Q*-switching operation was obtained at both 1.3 and 2 μm. The pulse width of 32 ns was achieved at 1.3 μm with repetition rate of 44 kHz, single pulse energy of 51.9 μJ, and output power of 425 mW. Meanwhile, 510 ns and 92 kHz pulses with energy of 36.1 μJ and output power of 2.48 W were obtained at 2 μm. This work provides the potential of liquid metal for improving metal functions and flexible optical devices.

Keywords: GaInSn nanosphere; passively Q-switched lasers; saturable absorber.
doi: 10.3788/COL202018.111901.

Nanosecond *Q*-switched lasers play important roles in many fields, such as spectroscopy, biomedical research, and laser radar, due to the advantages of short pulse width and high pulse energy[1–5]. Possessing compact structure and low cost, passively *Q*-switched lasers have stirred up particular interests for high-speed photonics and on-chip integration. One of the key components of passively *Q*-switched lasers is the saturable absorber (SA). Recently, two-dimensional (2D) materials such as graphene[6], transitional metal dichalcogenide[2,7,8], and black phosphorous[9] have been widely investigated as SAs for their ultra-thin nature and superior properties such as broadband absorption, fast nonlinear response, and high third-order nonlinearity. A variety of *Q*-switched and mode-locked lasers with 2D materials as SAs have been demonstrated, with pulse duration over a wide range from nanosecond to femtosecond levels[2,6–16]. Although these excellent results clearly reflect diverse properties of the 2D crystalline materials, the problems such as significant crystal defects in growth of atomically thin layers, structural phase instability under laser illumination, low yield, as well as weak absorption per layer have become annoying shortcomings that may hinder their applications. Motivated by the purpose for overcoming these distinctive obstacles of 2D crystals, a lot of efforts have been devoted to exploit the plasmonic effect of zero-dimensional metal nanoparticles (NPs).

The recent investigation of zero-dimensional NPs, including nanospheres, nanocubes, and quantum dots, provides a new approach to nonlinear photonics, thanks to their unique localized surface plasmon resonance (LSPR) effect originating from the quantum confinement in three dimensions and large surface-to-volume ratio[17]. When metal NPs are stimulated by light, the surface free electrons oscillate with the electric field of light, and, meanwhile, the polarizability experiences a resonant enhancement. Consequently, the dipole electric field in NPs is greatly enhanced, exhibiting a strong third-order nonlinear optical effect. Metal NPs have been widely applied in nonlinear optics currently[3,4,13,18]. For example, Au NPs have a large third-order nonlinear coefficient (10^{-6} esu)[13]. Various passively *Q*-switched solid-state lasers modulated by Au NPs have been successfully explored at different wavelengths from 605 nm to 3 μm[1,3,13,19,20]. Other than Au, a Ag NPs-based *Q*-switched laser has also been demonstrated at 2 μm[4]. However, these noble metals showed disadvantage of high cost that may gradually limit the motivation for further research.

GaInSn, a typical liquid metal at room temperature, has been considered as an intriguing combination of metallic and fluidic properties[21]. GaInSn has the advantages of low cost, high thermal conductivity, nontoxicity, and shape-reconfigurability[22–24] and has been applied for flexible biosensors[25], coolant in heat transfer[26], superconductivities[21], etc. However, most researchers focused on the electronic and thermal conductivity due to its excellent performance in these respects. Nonlinear optical properties of GaInSn, especially their performance as SAs in *Q*-switched pulse lasers, are still lacking.

Here, we firstly, to the best of our knowledge, reported the LSPR-induced saturable absorption properties of GaInSn nanospheres and their application in 1.3 and 2 μm passively *Q*-switched pulsed lasers. For the 1.3 μm laser, under the pump power of 4.7 W, 32 ns pulses were obtained with repetition rate of 44 kHz, output power of 425 mW, and single pulse energy of 51.9 μJ. For the 2 μm laser, under the pump power of 14 W, a pulse duration of 510 ns was obtained with repetition rate of 92 kHz, output power of 2.48 W, and single pulse energy of 36.1 μJ. Our work may promote the development of the metal

nanostructure SAs in the applications of optics and optoelectronics.

The GaInSn nanospheres were synthesized by the ultrasonic method. The precursors were firstly mixed with 67% Ga, 20.5% In, and 12.5% Sn and heated at 350°C for 10 min, and a GaInSn alloy was obtained. Then, the alloy was shattered into nanospheres by ultrasonication for 20 h in acetone. The photograph of the suspension of GaInSn nanospheres is shown in Fig. 1(a). The morphology of the nanospheres was characterized by scanning electron microscopy (SEM), as shown in Fig. 1(b). The average radius of the spheres was 86 nm, calculated by the size distribution, as illustrated in Fig. 1(c).

Energy dispersive X-ray spectroscopy (EDS) was performed to determine the microscopic stoichiometric ratio of Ga, In, and Sn, as depicted in Fig. 1(d). The characteristic peaks of Ga, In, and Sn are 1.09 eV, 3.28 eV, and 3.44 eV, respectively, which are clearly seen in the EDS spectra. The calculated normalized ratio from EDS is 62.7:25.0:12.2, slightly deviating from the feeding ratio, which may result from the oxidation of Ga. This confirms the unchanged alloy structure of GaInSn during the ultrasonication process.

In order to investigate the nonlinear optics properties of the as-prepared GaInSn nanospheres, an open-aperture Z-scan measurement was carried out by using a Ti:sapphire tunable femtosecond optical parametric amplifier (OPA) laser with a repetition rate of 76 MHz and a pulse width of 200 fs. The GaInSn nanospheres suspension was spin-coated on the CaF_2 substrates. The measurement results are shown in Fig. 2. The linear non-saturable loss of GaInSn nanospheres was 24% and 20% at 1.3 and 2 μm, respectively. According to the fitting curves, the extracted modulation depths ΔR were 2.6% and 9.3% at 1.3 and 2 μm, with the saturation intensity I_s of 5.19 and 2.13 MW/cm^2, respectively. This saturable absorption process can be regarded as LSPR-induced optical absorption, hot electron generation on the nanospheres, as well as hot electron cooling and recombination with the hole.

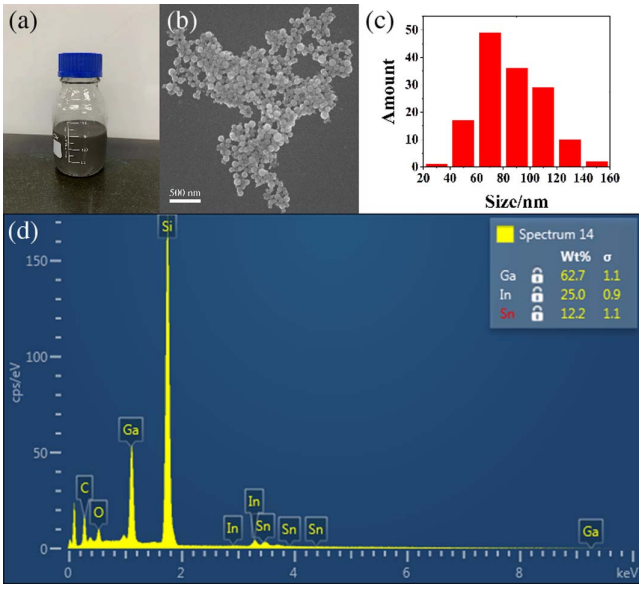

Fig. 1. (a) As-prepared suspension of GaInSn nanospheres. (b) SEM image. (c) Size distribution. (d) EDS spectrum.

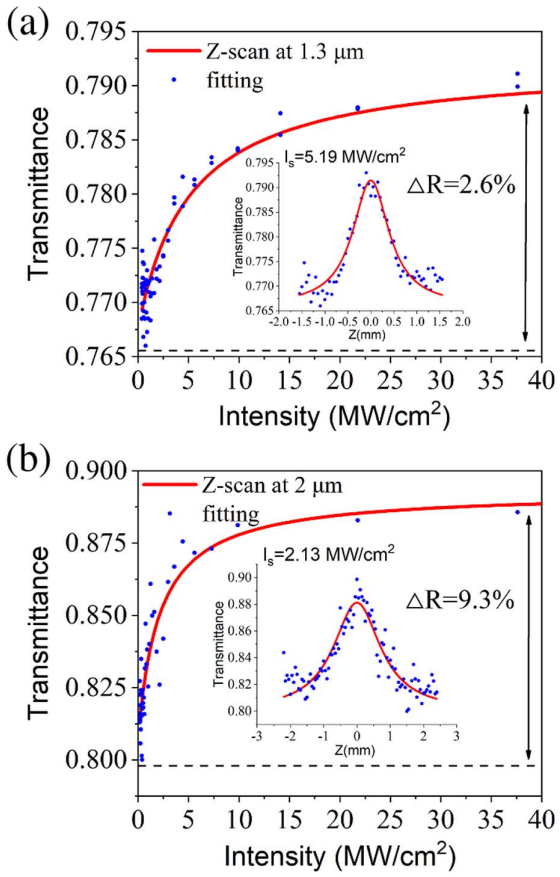

Fig. 2. Transmittance curve versus incident optical power intensity of GaInSn nanospheres at (a) 1.3 and (b) 2 μm. The typical Z-scan results are shown in the insets.

Subsequently, we performed a passively Q-switched laser with GaInSn nanospheres SAs at 1.3 and 2 μm. The corresponding experimental setup is shown in Fig. 3. For the 1.3 μm laser, a compact plano-concave cavity

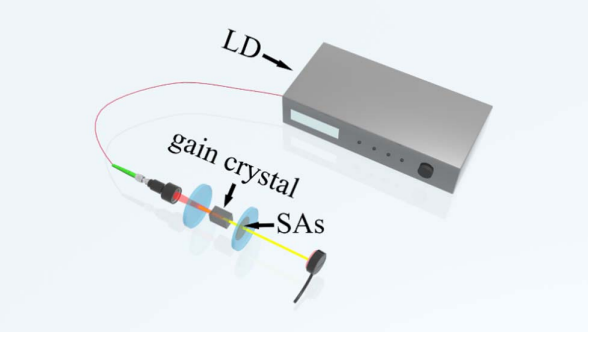

Fig. 3. Experimental setup of passively Q-switched laser with GaInSn nanospheres as SAs.

pumped by a fiber coupled 808 nm laser diode (LD) was employed. The total cavity length was fixed to 27 mm. An a-cut, 0.3% (atomic fraction) Nd:YVO_4 was used as the gain medium, which was surrounded by a copper heat sink and cooled by circulating water at ~20°C. The input coupler was a concave mirror with a curvature radius of $R = -100$ mm and high-transmission (HT) coated at 808 nm and high reflection (HR) at 1.3 μm. The output coupler was a plane mirror with a transmission of 10% at 1.3 μm. The cavity for 2 μm laser was also a plano-concave construction with a length of 27 mm. An a-cut, 3% Tm:$YAlO_3$ (Tm:YAP) was placed in the cavity as gain medium and pumped by a 795 nm LD. The length of both Nd:YVO_4 and Tm:YAP is 8 mm. The input mirror ($R = -500$ mm) was HT coated at 795 nm and HR coated at 2 μm. The output mirror was a plane mirror with a transmission of 5% at around 2 μm. GaInSn nanosphere SAs were applied by spin-coating the prepared dispersions on the two output couplers.

When increasing the pump power, the output powers of continuous wave (CW) and Q-switching (QS) at both wavelengths are shown in Fig. 4. Under the absorbed pump power of 4.19 W, the maximum CW output power at 1.3 μm was 0.91 W, and the slope efficiency was 31.3%.

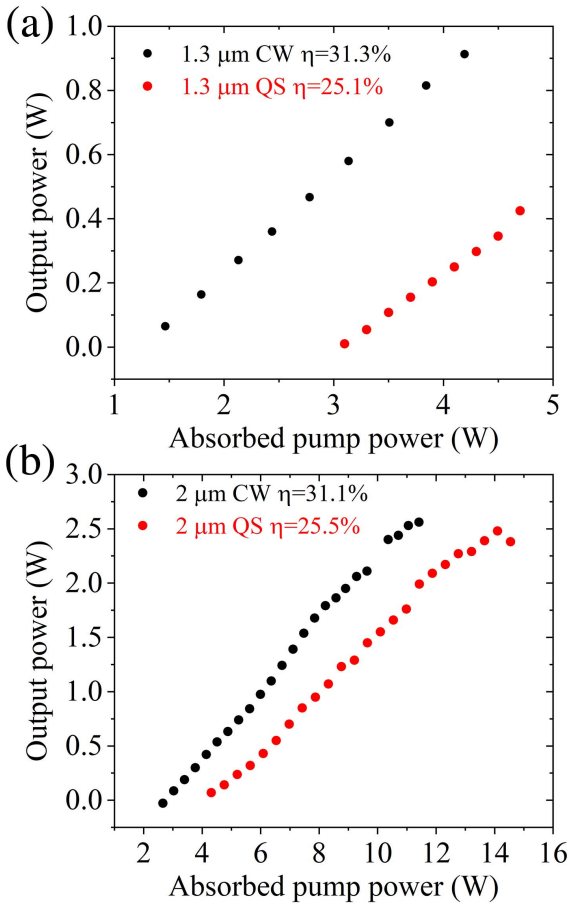

Fig. 4. Dependence of continuous-wave (CW) and Q-switching (QS) output power on absorbed pump power at (a) 1.3 and (b) 2 μm.

For 2 μm, the maximum CW output power of 2.56 W was obtained at pump power of 11.4 W, and the slope efficiency is 31.1%. When the GaInSn SAs were inserted into the cavity, QS operation was achieved. The QS output power increased monotonically and linearly with the absorbed pump power and reached 425 mW at a pump power of 4.7 W at 1.3 μm. At 2 μm, the maximum QS output power of 2.48 W was obtained at pump power of 14.1 W. By linear fitting, the slope efficiencies were 25.1% and 25.5% at 1.3 and 2 μm, respectively, which are higher than that of graphene SAs at 1.3 μm (21%)[27] and Au nanorods SAs at 2 μm (8.6%)[1]. It indicates a lower resonator loss level for our laser configuration, maybe benefiting from laser crystals of high emission cross section, good cavity design with mode matching between pump and resonation modes, as well as appropriate loss of GaInSn SAs.

Fig. 5 shows the dependence of pulse duration and repetition rate on the pump power at 1.3 and 2 μm. At 1.3 μm, by increasing the pump power from 3.1 to 4.7 W, the repetition rate increased rapidly from 6 to 44 kHz, while the pulse duration dropped from 133 to 32 ns. For 2 μm, the repetition rate rose drastically from 3.7 to 73 kHz with pump power changing from 4.3 to 7.8 W and then increased slowly when the pump power exceeded 7.8 W. The pulse duration dropped quickly from 5.5 to 1.22 μs with pump power varying from 4.3 to 7.8 W. Then, the decrease slowed down to the minimum pulse duration of 510 ns at a pump power of 14.1 W, which should result from the full saturation of SAs. This phenomenon is in good accordance with the general rule of passively QS

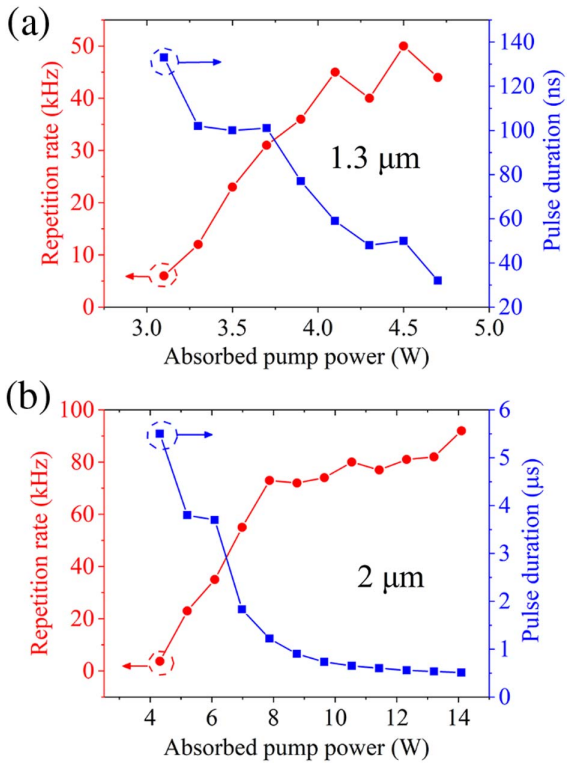

Fig. 5. Pulse duration and repetition rate variation with increasing pump power at (a) 1.3 and (b) 2 μm.

where pulse duration will rapidly decrease with increasing pump power but tends to saturation under relatively high pump, as testified by a variety of previous work[1,4,27]. For our 1.3 μm case shown in Fig. 5(a), limited by the maximum power of the 808 nm LD (<5 W), the intracavity intensity on the SAs is not enough to fully saturate it, so the pulse duration only exhibits a rapid decrease. For the 2.0 μm laser as in Fig. 5(b), both the rapid decrease region under the pump power less than 8 W and saturation region under higher pump power can be observed.

In addition, a typical *Q*-switched pulse train was recorded under the pump power of 4.7 W for 1.3 μm and 14 W for 2 μm, as shown in Fig. 6. For 1.3 μm, 32 ns of pulse duration was obtained with a repetition rate of 44 kHz and an output power of 425 mW, giving a pulse energy of 51.9 μJ, which showed a better performance than that of a passively *Q*-switched $Nd:GdVO_4$ laser with few-layered graphene as SAs (450 ns, 2.5 μJ)[27]. The corresponding pulse train and single pulse shape are shown in Fig. 6(a). For comparison, 510 ns pulses at 2 μm were achieved with the repetition rate of 92 kHz, output power of 2.48 W, and pulse energy of 36.1 μJ, as shown in Fig. 6(b). This result is better than those of the passively *Q*-switched Tm-doped fiber laser based on MoS_2 SAs (1.76 μs, 1 μJ)[28] and passively *Q*-switched $Tm:Y_3Al_5O_{12}$ (Tm:YAG) lasers based on Au nanorods SAs (796 ns, 380 mW) at 2 μm[1]. The shorter pulse duration of 1.3 μm than that of 2 μm should be attributed to the much longer relaxation time of $Nd:YVO_4$ ($7.6\times10^{-19}\,cm^2$ at 1.3 μm) versus Tm:YAP ($5\times10^{-21}\,cm^2$ at 2 μm) and, thus, a stronger laser energy storage.

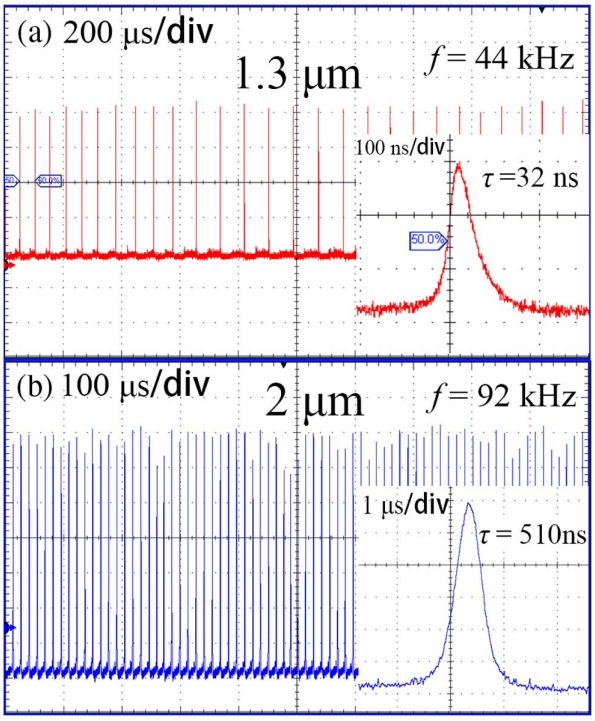

Fig. 6. Typical temporal pulse trains of *Q*-switched lasers operating at (a) 1.3 and (b) 2 μm with GaInSn nanospheres SAs.

In order to characterize the stability of QS, clock amplitude jitter (CAJ) was calculated, which is defined as the ratio of the standard deviation (σ) to the mean value (M) of pulse peak intensity[29]:

$$\mathrm{CAJ}=\frac{\sigma}{M}\times 100\%. \tag{1}$$

The CAJ of the pulse train in the Fig. 6 was 2.4% and 4.4% at 1.3 and 2 μm, respectively, which elucidates a good stability of the QS operation.

In conclusion, GaInSn nanospheres SAs were fabricated by the ultrasonic method with uniform shape and with diameter of about 86 nm. SEM and EDS were performed to characterize the morphology and the stoichiometry ratio of synthesized GaInSn. The GaInSn nanospheres exhibit strong surface plasmon oscillation strength, enabling progressive capabilities for laser modulation across a broad spectral range as attested in Z-scan measurement. Stable passively *Q*-switched lasers using GaInSn as SAs were achieved at 1.3 and 2 μm with the shortest pulse duration of 32 ns and 510 ns, respectively. Our experiments may shed light on the exploitation of novel metal nanostructures in the application of optics and optoelectronics.

This work was supported by the National Key R&D Program of China (Nos. 2017YFA0303700 and 2019YFA0705000), the National Natural Science Foundation of China (Nos. 11774161, 51890861, 11690031, 11627810, and 11674169), the Key R&D Program of Guangdong Province (No. 2018B030329001), and the Leading-edge Technology Program of Jiangsu Natural Science Foundation (No. BK20192001).

References

1. H. Huang, M. Li, P. Liu, L. Jin, H. Wang, and D. Shen, Opt. Lett. **41**, 2700 (2016).
2. Y. Huang, Z. Luo, Y. Li, M. Zhong, B. Xu, K. Che, H. Xu, Z. Cai, J. Peng, and J. Weng, Opt. Express **22**, 25258 (2014).
3. D. Wu, J. Peng, Z. Cai, J. Weng, Z. Luo, N. Chen, and H. Xu, Opt. Express **23**, 24071 (2015).
4. H. Ahmad, M. Samion, A. Muhamad, A. Sharbirin, and M. Ismail, Laser Phys. Lett. **13**, 126201 (2016).
5. M. Skorczakowski, J. Swiderski, W. Pichola, P. Nyga, A. Zajac, M. Maciejewska, L. Galecki, J. Kasprzak, S. Gross, A. Heinrich, and T. Bragagna, Laser Phys. Lett. **7**, 498 (2010).
6. L. Zhang, G. Wang, J. Hu, J. Wang, J. Fan, J. Wang, and Y. Feng, IEEE Photon. J. **4**, 1809 (2012).
7. H. Liu, A. Luo, F. Wang, R. Tang, M. Liu, Z. Luo, W. Xu, C. Zhao, and H. Zhang, Opt. Lett. **39**, 4591 (2014).
8. B. Chen, X. Zhang, K. Wu, H. Wang, J. Wang, and J. Chen, Opt. Express **23**, 26723 (2015).
9. A. A. Latiff, M. F. M. Rusdi, Z. Jusoh, M. Yasin, H. Ahmad, and S. W. Harun, Optoelectron. Adv. Mater. Rapid Commun. **10**, 801 (2016).
10. H. Ahmad, Z. Tiu, and S. Ooi, Chin. Opt. Lett. **16**, 020009 (2018).
11. T. Tang, F. Zhang, M. Wang, Z. Wang, and X. Xu, Chin. Opt. Lett. **18**, 041403 (2020).
12. Z. Du, T. Zhang, Z. Xie, J. Ning, X. Lv, J. Xu, and S. Zhu, Chin. Opt. Lett. **17**, 121404 (2019).

13. W. Duan, H. Nie, X. Sun, B. Zhang, G. He, Q. Yang, H. Xia, R. Wang, J. Zhan, and J. He, Opt. Lett. **43**, 1179 (2018).
14. X. Jiang, S. Liu, W. Liang, S. Luo, Z. He, Y. Ge, H. Wang, R. Cao, F. Zhang, Q. Wen, J. Li, Q. Bao, D. Fan, and H. Zhang, Laser Photon. Rev. **12**, 1700229 (2018).
15. H. Zhang, Q. Bao, D. Tang, L. Zhao, and K. Loh, Appl. Phys. Lett. **95**, 141103 (2009).
16. H. Zhang, S. Lu, J. Zheng, J. Du, S. Wen, D. Tang, and K. Loh, Opt. Express **22**, 7249 (2014).
17. F. Nucciarelli, I. Bravo, S. Catalan-Gomez, L. Vazquez, E. Lorenzo, and J. Pau, Nanomaterials **7**, 172 (2017).
18. D. Miu and I. Nicolae, Thin Solid Films **697**, 137829 (2020).
19. S. Wang, Y. Zhang, J. Xing, X. Liu, H. Yu, A. Di Lieto, M. Tonelli, T. Sum, H. Zhang, and Q. Xiong, Appl. Phys. Lett. **107**, 161103 (2015).
20. H. Zhang and J. Liu, Opt. Lett. **41**, 1150 (2016).
21. T. Mochiku, M. Tachiki, S. Ooi, and Y. Matsushita, Physica C **563**, 33 (2019).
22. T. Liu, P. Sen, and C. Kim, J. Microelectromech. Syst. **21**, 443 (2012).
23. M. Dickey, ACS Appl. Mater. Interfaces **6**, 18369 (2014).
24. M. Dickey, R. Chiechi, R. Larsen, E. Weiss, D. Weitz, and G. Whitesides, Adv. Funct. Mater. **18**, 1097 (2008).
25. M. Ou, W. Qiu, K. Huang, H. Feng, and S. Chu, ACS Appl. Mater. Interfaces **12**, 7673 (2020).
26. H. Liu, Y. Shao, Z. Chen, and Z. Xie, Int. J. Therm. Sci. **144**, 129 (2019).
27. J. Xu, X. Li, J. He, X. Hao, Y. Yang, Y. Wu, S. Liu, and B. Zhang, Opt. Lett. **37**, 2652 (2012).
28. Z. Luo, Y. Huang, M. Zhong, Y. Li, J. Wu, B. Xu, H. Xu, Z. Cai, J. Peng, and J. Weng, J. Lightwave Technol. **32**, 4679 (2014).
29. J. Xu, Y. Sun, J. He, Y. Wang, Z. Zhu, Z. You, J. Li, M. Chou, C. Lee, and C. Tu, Sci. Rep. **5**, 14856 (2015).